A POLARIMETER FOR NUCLEONS BETWEEN 100 AND 500 MeV

G. WATERS*

Rutherford Laboratory, Chilton, Oxon, England

I. M. BLAIR

Atomic Energy Research Establishment, Harwell, England

G. A. LUDGATE*, N. M. STEWART

Bedford College, University of London, England

C. AMSLER, R. C. BROWN†, D. V. BUGG, J. A. EDGINGTON,
C. J. ORAM*, K. SHAKARCHI

Queen Mary College, University of London, England

A. S. CLOUGH

University of Surrey, Guildford, England

and

D. AXEN, S. JACCARD† and J. VÁVRA§

University of British Columbia, Vancouver, Canada

A polarimeter is described having a large solid angle of acceptance and using a carbon analyser combined with 12 multi-wire proportional chambers. Its analysing power for protons has been calibrated at TRIUMF with an absolute accuracy reaching $\pm 0.015 = 2\%$ in the angular range 3.5° to 28° laboratory angle and for incident energies between 107 and 462 MeV. A mean analysing power of about 35% and an efficiency of approximately 3% was observed.

1. Introduction

A carbon polarimeter with a large solid angle of acceptance has been constructed for studies of the spin dependence of the nucleon–nucleon interaction. It has proved a very convenient and precise instrument, and has been used in a series of experiments at the TRIUMF 520 MeV cyclotron. Using it the Wolfenstein parameters P, D, R and R' have been measured in p–p elastic scattering[1] and in addition R_t for the reaction D(p, n) has been determined during the setting up of a polarised monoenergetic neutron beam[2]. The polarimeter is at present being utilised in an extensive series of measurements of Wolfenstein parameters in n–p elastic scattering[3,4,5].

The polarimeter consists essentially of a carbon scatterer, 53×53 cm^2 and up to 6 cm thick, sandwiched between six multi-wire proportional chambers 50×50 cm^2 and a further six 100×100 cm^2. In the energy range accessible at TRIUMF carbon is a very suitable analyser as it has a large analysing power, large scattering cross section and is conveniently available in slabs of varying thickness. This polarimeter does not distinguish between elastic and inelastic scattering from carbon, and had, therefore, to be calibrated in proton beams of known energy and polarisation. Details of this calibration (see also ref. 6) will be given, since it appears to be a characteristic of carbon, and insensitive to details of the chambers. The calibration has been made with an absolute accuracy of about ± 0.015 using protons with incident energies in the range 107 to 462 MeV. The calibration was performed with a polarised proton beam produced by scattering an unpolarised proton beam from liquid hydrogen. The polarisation of these protons was established with an absolute accuracy of ± 0.003 to 0.01 in a double scattering experiment reported elsewhere[7].

---

* Now at the University of British Columbia.
† Now at the Rutherford Laboratory, Chilton, Oxon, England.
· Now at SIN, Villigen, Switzerland.
§ Now at Carleton University, Ottawa, Canada.

2. The polarimeter

The layout of the polarimeter in the experimental area is shown schematically in fig. 1 in the configuration used during its calibration. Incident protons are defined by the six half metre square multi-wire proportional chambers which have sense wires alternately vertical and horizontal. After the scatter in carbon exit tracks are defined by the six one metre square chambers. Three chambers are used in each plane, front and back, to incorporate redundancy, so as to achieve high efficiency and reliability with the minimum of instrumental asymmetries due to chamber inefficiencies. The carbon is mounted in a frame which may slide out laterally, thereby allowing the use of unscattered particles to check the alignment of the polarimeter. The chambers may be moved easily along the length of the polarimeter, which allows for variable geometry. The polarimeter was used with the front chambers equally spaced 358 mm apart and the back ones 287 mm apart, although these spacings are not critical. The electronic logic is triggered by scintillation counters S3, S4 and S5, each 3 mm thick, and also by S6 6 mm thick. Counters S4 and S5 are nearly touching the carbon and comprise part of the analyser. They, as well as S3, are composed of four similar scintillators separately wrapped and butted together. Counter S6 consists of six separate scintillators. This subdivision results in improved efficiency and gives some crude positional information in addition to that from the chambers. The detectors are mounted on a strong rigid carriage, 3.5 m long by 1.6 m wide, which also carries the gas manifold, power supplies, preamplifiers and readout electronics for the chambers. The whole instrument weighs 3 t and moves freely on four wheels. The carriage is equipped with survey marks and liquid level sensors which allow its repositioning with a precision of ±1 mm in three dimensions. By the use of a two-point suspension system, operating on a carefully machined and surveyed track, the chambers themselves may be aligned with a relative precision approaching ±0.1 mm.

The construction of the chambers follows the precedent set by Charpak et al.[8] with 20 μm diameter gold plated tungsten sense wires forming a plane sandwiched between two EHT planes of 0.12 mm diameter beryllium–copper wire. The spacing between EHT wires is 2 mm, as is the sense wire spacing. However, for the latter, adjacent wires are connected in pairs, giving a 4 mm

channel spacing which reduces electronic hardware costs. The high voltage and sense wire planes are 8 mm apart and the complete assembly is mounted in a gas-tight envelope closed by 0.1 mm mylar sheets. The sense wires are mechanically supported by 1 mm diameter copper wires enclosed in PVC insulation; the small chambers have a single pair of support wires at their centre, and the large chambers two equally spaced pairs of support wires. With the chambers operating at 5.8 to 6.0 kV the support wires are maintained at 2.6 kV to avoid creating an inefficient region in their vicinity. The gas filling is essentially the magic-gas mixture[9] containing 0.3% of freon 13 B1* and bubbled through di-methoxymethane (methylal) to reduce the deleterious effects[10] of hydrocarbon accumulation on the sense wires. After three years of intensive use a small build up of carbon deposits can be noticed as a slight darkening of some of the sense wires, but this is in no way a serious problem as yet. Optimum performance is obtained with an argon to isobutane ratio between 2.3 and 3.0 to 1 and maintaining a gas flow of 50 cm³ min⁻¹ per chamber.

A sequential readout system[11] is used, interfacing via CAMAC to a PDP-11 computer. The electronic scheme is shown in outline in fig. 2. The hierarchy of channel addresses, indicated in fig. 2b, enables the readout signal to be routed by the chamber control unit to only those second-stage encoder units containing active information. Thus the readout time is a constant independent

---

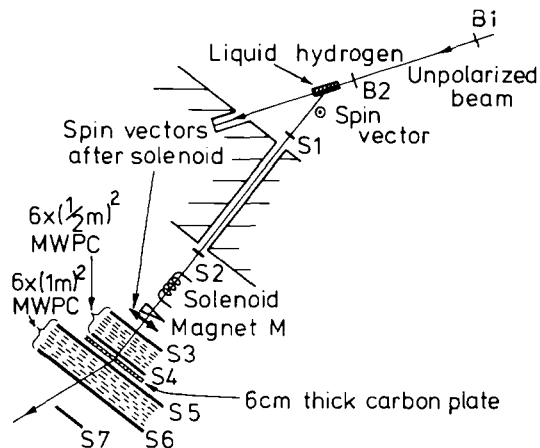* Dow Chemical registered trade name.

Fig. 1. Schematic layout of the experimental area for the calibration of the polarimeter. B1 and B2 are monitors for centring the extracted beam on the liquid hydrogen target.
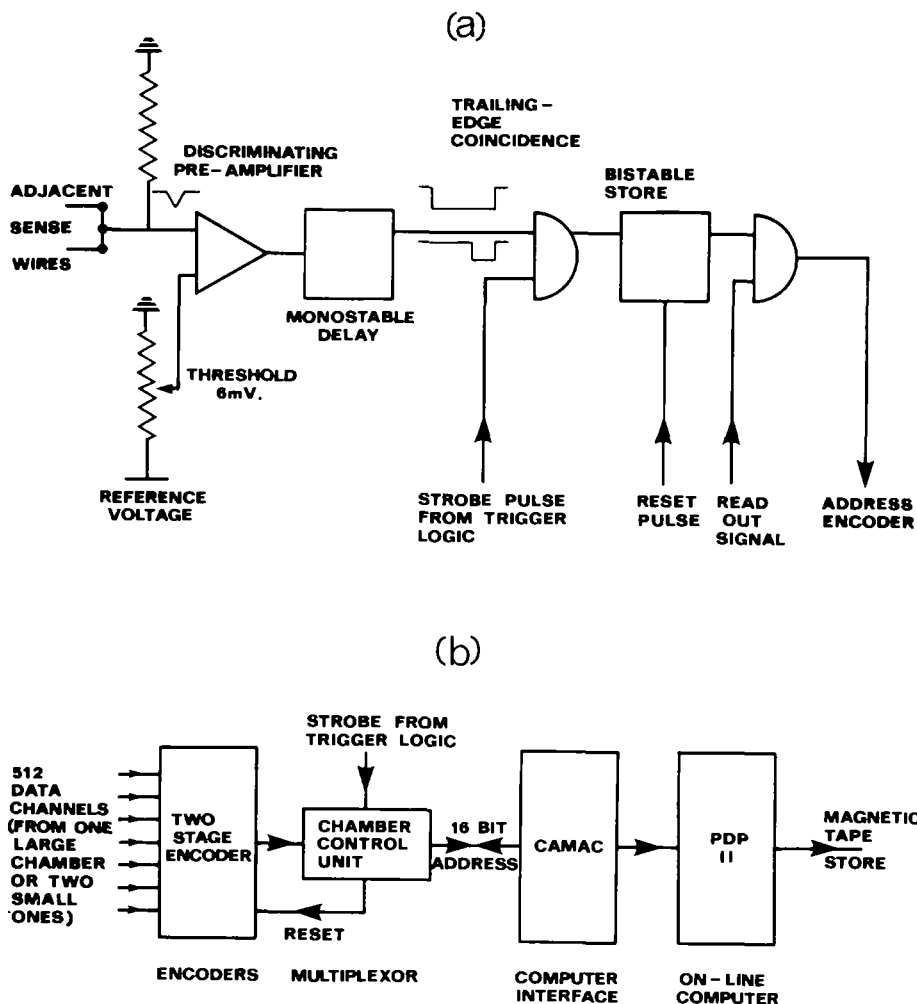
Fig. 2. a) Electronic logic for one MWPC channel; b) Organization of the data highway.

of channel position, and is equal to approximately 2 μs per channel fired. The total dead time, including CAMAC operations and writing onto tape, was about 2 ms during the calibration experiment described here, allowing near to 200 events per second to be recorded. With 6 cm thickness of carbon, and the incident beam, as here, centred on the polarimeter approximately 1 proton in 14 undergoes a useful scatter. If the incident particles are uniformly distributed over the carbon, as in our n–p experiment, about 1 proton in 30 undergoes a useful scatter.

The detection efficiency of the chambers at their operational optimum approaches 99.9%, the residual inefficiency being attributable mainly to timing jitter in the trailing-edge coincidence unit, fig. 2a. About 95% of the time only one channel fires in

a chamber. Some particle tracks, particularly those highly inclined to the normal to the sense wires, cause adjacent channels to fire, and these comprise about 4% of all events. The remaining <1% of events exhibit a Poisson distribution of multiplicities, indicating the random nature of the noise pulses. The total dark current is generally <0.1 μA per chamber, corresponding to a noise rate of the order of 25 noise pulses per metre wire per second.

3. Data acquisition

It was possible to subject each event to up to four on-line tests by the PDP-11 computer before it was written onto tape.
a) A window could be applied to the time of flight between either an external scintillator

(here S1) or the cyclotron RF and the scintillator S5. Times of flight measured by S1, S2, S5 and the cyclotron RF were recorded with every event for tighter off-line analysis.

b) Events with scattering angles less than any chosen amount, usually 3.5°, could be rejected; the equal spacing of chambers simplifying the software logic, which operated only on information concerning the wire coordinates and was independent of external scintillation counter requirements.

c) An event could be rejected if two out of three chambers in either plane, before or after the carbon, had a multiplicity greater than one. The intention of this test was to clean up the sample of events recorded. However, it has been found undesirable, since it leads to a narrow plateau in chamber performance: at low E.H.T. the efficiency for a single signal drops, and at high E.H.T. the efficiency drops because two neighbouring wires fire. What is worse, the precise plateau point changes with track inclination, leading to lower efficiency in the corners of the rear chambers and an azimuthal inefficiency of the form cos(4Φ) (see section 5).

d) The bit pattern of the trigger scintillators S3 to S6 could be checked to eliminate two or more simultaneous particles in the polarimeter.

Histograms of time of flight spectra, counter bit patterns, chamber wire patterns and multiplicities could be inspected at any time during the data-taking on a Tektronix 4010 visual display unit.

4. Calibration

The calibration was a double scattering measurement in which the unpolarised proton beam, extracted from the TRIUMF cyclotron, was polarised by elastic scattering from hydrogen at 24° lab. and then analysed by a second scatter in carbon.

Let P be the magnitude of the polarisation produced by the scatter in hydrogen. Its direction was initially normal to the plane of this scatter, vertically upwards, and it was rotated into the horizontal direction **h** by a solenoid in the secondary beamline, fig. 1. Let I and I_0 be the polarised and unpolarised cross sections in carbon, and **k**, **k′** be unit vectors parallel to tracks entering, leaving the carbon. Then

$$I(\theta, \Phi) = I_0(\theta) \left[1 + PA_c(\theta) \cos \Phi\right], \tag{1}$$

where θ is the polar angle of scatter in carbon, $A_c(\theta)$ is the analysing power of carbon, and

$$\cos \Phi = \mathbf{h} \cdot \mathbf{n},$$

with

$$\mathbf{n} = \frac{\mathbf{k} \times \mathbf{k'}}{|\mathbf{k} \times \mathbf{k'}|}.$$

The distribution, $f(\theta, \Phi)$ of events observed in the polarimeter was such that

$$f(\theta, \Phi) \propto \left[1 + \varepsilon(\theta) \cos \Phi\right] D(\theta, \Phi), \tag{2}$$

where $\varepsilon(\theta) = PA_c(\theta)$ is the magnitude of the asymmetry and $D(\theta, \Phi)$ is the detection efficiency of the polarimeter. A direct determination of the Φ dependence of D is made by averaging over alternate runs in which **h** was reversed by means of the solenoid.

The polarisation P has been determined in a separate double scattering experiment, in which the carbon polarimeter was replaced by one detecting elastic p–p scatters at 24° lab. from a polyethylene target[7]).

4.1. EXPERIMENTAL LAYOUT

The layout is shown in fig. 1. The extracted beam of TRIUMF, variable in energy from 200 to 516 MeV (known to a precision of ± 1 MeV at each energy from the measured cyclotron field) was focussed to ≤ 8 mm full width at half maximum at a liquid hydrogen target which was of diameter 5.1 cm and length 20.6 cm. Scattered beams were taken off at 24° lab. and also at 15° lab. for the calibration at the highest energy. These angles are close to the maximum of the polarisation in p–p elastic scattering[1]). The secondary beams emerged through a 25 t lead and steel collimator, having eleven equally spaced ports of length 3.5 m. These collimator ports, designed for subsequent work with neutrons, have diameters of 100 mm and 125 mm in their upstream and downstream sections. A scintillation counter telescope S1, S2 in conjunction with the front chambers defined a beam passing cleanly through the collimator without striking the walls. The scintillator S1 was 2.5 cm diameter, and S2 was 5.1 cm diameter. Time of flight between S1 and S5 separated most of the pions in the beam and all of the lower energy protons produced by inelastic scattering in the liquid hydrogen. At the higher energies, about 1% of surviving particles were pions with the same velocity as elastic protons, but one-seventh of the momentum; these were readily identified

and removed by their angle of deflection in the small steering magnet M, which deflected elastic protons by 7 mrad. A veto counter S7, 35.6 cm in diameter, was positioned so as to eliminate most of the multiple Coulomb scattering in carbon, which was particularly serious at low energy. This counter rejected most events with a scattering angle $\gtrsim 3.5°$.

The superconducting solenoid[12]) is 1 m long with an inside diameter of 10 cm. It is capable of a field of 6 T at an excitation current of 212 A. The consumption of liquid helium was on average 1.5 l/h. The field of the solenoid has been calculated, and experimentally checked, to a precision of better than 1%.

The liquid hydrogen target, designed also as a liquid deuterium target for producing neutrons[13]), was cooled by a Phillips B-20 cryogenator. The target had end windows 50 μm thick, which produced a background of near 0.5% of elastic protons from the hydrogen. An evacuated flask of identical construction, mounted underneath the target, could be rapidly raised into the beam in order to measure the count rate needed for background subtraction.

5. Data analysis

Tracks were separately fitted to the front and rear chamber coordinates and then checked to ensure that the incoming and outgoing trajectories met at the carbon (or S4 or S5), within errors. Multiple wires firing in the chambers were incorporated into the fitting procedure by using a least squares method to generate straight lines through the various coordinates, and taking that line which gave the best fit.

A test was made on the exit track to ensure that it would be accepted geometrically at its given polar angle θ, whatever the azimuthal angle Φ. That is, the trajectory of the scattered proton was rotated about that of the incident proton, and it was required that the entire circumference of the resulting cone intercepted the back trigger counters S5 and S6, while missing the veto counter S7. Thus the detection efficiency $D(\theta, \Phi)$ is close to unity for all θ, Φ and depends only on chamber efficiency.

Accepted events were binned into 2° intervals of θ, and the distribution of events was fitted by expanding the detection efficiency $D(\theta, \Phi)$ in eq. (2) as a Fourier series:

$$f(\theta, \Phi) = N(\theta) \left[1 + \varepsilon(\theta) \cos \Phi \right] \times$$

$$\times \left[\alpha_0 + \sum_{n=1}^{16} \{\alpha_n(\theta) \cos n\Phi + \beta_n(\theta) \sin n\Phi\} \right] \tag{3}$$

Here N is the total number of events at an angle θ. The coefficients α_n and β_n, which describe the detection efficiency, were determined by averaging over f^- and f having opposite spin orientation h. Taking the difference between f^+ and f, and expanding eq. (3) in terms of $\cos n\Phi$ and $\sin n\Phi$, one finds from eq. (3):

$$\langle\cos \Phi\rangle^+ - \langle\cos \Phi\rangle^- = \varepsilon\left(1 + \frac{\alpha_2}{2\alpha_0} - \frac{\beta_1^2}{2\alpha_0^2}\right) + O(\varepsilon^3). \tag{4}$$

The term of order ε^3 was always negligible, and the term $-\varepsilon\beta_1^2/2\alpha_0^2$ almost always so, but not the term involving α_2. This is given by

$$\langle\cos 2\Phi\rangle^+ + \langle\cos 2\Phi\rangle^- = \alpha_2/\alpha_0. \tag{5}$$

It arises from differences in efficiency in the horizontal and vertical planes.

We have found that the coefficient α_4 was a sensitive monitor of the health of the chambers, particularly for $\theta \geqslant 16°$. The corners of the $1 \times 1 \text{ m}^2$ chambers received highly inclined tracks, tending to lead to high multiplicities. When test 3(c) was applied on-line, limiting the multiplicity in two out of three chambers to 1, this effect was particularly serious, and for this reason the test has been discontinued. Fortunately α_4 does not have any direct bearing on the determination of $\varepsilon(\theta)$. We have confirmed in runs without 3(c) that the calibration was unaffected.

The tiny subtraction for background from the empty hydrogen target was not made channel by channel as this would merely introduce statistical noise. Instead, it was assumed that the θ dependence of ε was the same for events from the full (F) and empty (E) targets, but that the polarisation P of beam particles may have been different. The weighted mean ($\bar{\varepsilon}$) of ε over θ was formed, using as weighting factor for each bin $N(\theta)\varepsilon^2(\theta)$. Then if B was the fraction of events originating from the empty target, and $R = \bar{\varepsilon}_E/\bar{\varepsilon}_F$ was the ratio of mean asymmetries from target empty and full, the corrected asymmetry was given by

$$\varepsilon = \varepsilon_F(1 - BR)/(1 - B)$$

$$\approx \varepsilon_F[1 - B(R-1)]. \tag{6}$$

In practice, $R \approx 0.5$ and the correction was $\leqslant 25\%$ of statistical errors on target full data.

Finally, at low energies, some bins for $\theta \leqslant 7°$ were discarded because of contamination by multiple Coulomb scattering in the carbon. The onset of multiple scattering was conspicuous, since $N(\theta)$ rose dramatically at small θ. In principle, one could have accepted these events, but in practice we wished in parameterising the results to make use of the well known fact that for nuclear scattering, both elastic and inelastic, $\varepsilon(\theta) \propto \theta$ as $\theta \to 0$.

6. Results and discussion

Approximately 8×10^5 scatters in carbon were recorded for each of 9 energies at 24° scattering angle from hydrogen using a 6 cm thick carbon slab; also for the highest energy at 15° with 6 cm of carbon, and for 4 low energies at 24° using 3 cm of carbon. We were prepared to find that the analysing power of carbon depended significantly on the thickness of carbon, either because of double
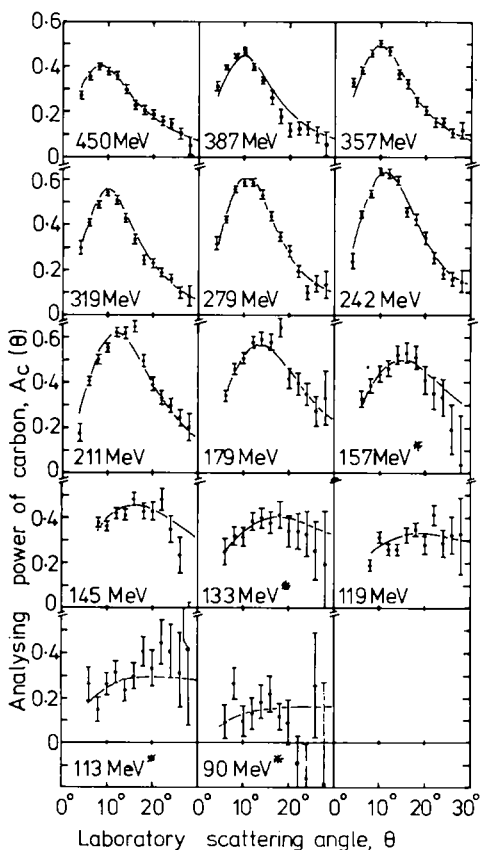

Fig. 3. Data from this experiment at 14 energies; continuous lines are our empirical fit. The energies given are those at the centre of the carbon, whose thickness was 6 cm except at the asterisked energies, when 3 cm was used.

scattering, or because of the range of protons leaving the carbon. The latter effect should have been biggest at low energies. However, from an overlap between two sets of data with 3 cm, and two sets with 6 cm, of carbon we found no discernable difference if the analysing power was taken to be a function of the momentum at the centre of the carbon. It therefore seems likely that the results we have obtained will be generally applicable to other instruments not too different in geometry. These results are shown in fig. 3.

We have found it convenient to parameterise the results for the purpose of interpolation in angle and energy by an empirical fit:

$$A_c(p, \theta) = \frac{a(p)\, P_T}{1 + b(p)\, P_T^2 + c(p)\, P_T^4}$$

where $P_T = pR \sin \theta$, p is the momentum of the proton at the centre of the carbon in GeV/c, and $R = 13.922\,(\text{GeV}/c)^{-1}$ characterises the radius of the carbon nucleus. The coefficients a, b, and c are given by:

$$a(p) = a_0 + a_1 p + a_2 p^2 + a_3 p^3 + a_4 p^4,$$

$$b(p) = b_0 + b_1 p + b_2 p^2 + b_3 p^3,$$

$$c(p) = c_0 + c_1 p + c_2 p^2 + c_3 p^3 + c_4 p^4,$$

where the values of the coefficients are given in table 1. The errors on these coefficients are highly correlated and are therefore not given. The error on the fit is limited by the statistical error of the calibration, and is given as a function of energy in fig. 4.

In this calibration, no restriction has been placed on inelasticity in the scatter in the carbon, other than the range requirement that the exit protons reach S6. Our highest two energies overlap the
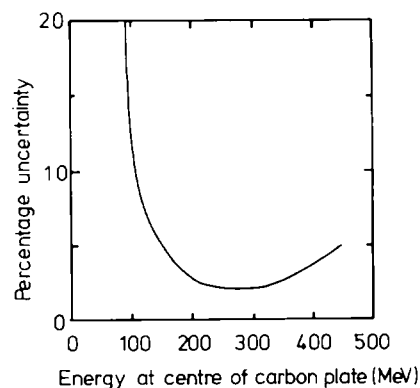

Fig. 4. The percentage uncertainty in our empirical fit as a function of energy at the centre of the carbon.

TABLE 1

Values of the coefficients for the empirical fit to the analysing power of carbon

Coeffi-cient	Value of index n				
	0	1	2	3	4
a_n	- 1.4612	3.9771	4.5465	14.691	7.9534
b_n	1.7526	- 4.4892	2.6525	0.19632	-
c_n	0.31303	- 2.498	6.5019	- 6.7049	2.3974

lowest two of the small angle data from CERN of Aebischer et al.[14]). This group determined A_c when the proton was allowed either unlimited inelasticity in the scatter on carbon, or an energy loss limited by a range energy telescope. Their results are shown in fig. 5 at an incident energy of 399 MeV with inelasticity $\leqslant 16$ MeV, and at 462 MeV with inelasticity $\leqslant 38$ MeV, together with the data unlimited in inelasticity at the same energies. The agreement of our results with the latter is good, and clearly verifies that the analysing power is reduced by highly inelastic events.

The characteristics of A_c in our energy range confirm the main trends of earlier data[14-17]. It peaks at a transverse momentum $p \sin \theta = 145$ MeV/c and an energy near 240 MeV. The broad maximum at the lower energies narrows to a forward peak as the energy increases, without any sign of a secondary minimum. This agrees with the well-known effect shown by Chesnut et al.[18] that inelastic scattering fills in the dip in the elastic scattering curve. A comparison of our data with the results of Chesnut et al. at 220 MeV shows this smoothing effect (fig. 6); the forward peak centred close to 16° is in good agreement.

At the highest energy, the improvement over the lowest energies of Eandi et al.[19] is shown in

Fig. 6. Comparison of our effective analysing power of carbon at the incident proton energy of 230 MeV (solid circles) with the elastic polarisation measurements of Chesnut et al. at 220 MeV (ref. 18, open circles).

fig. 7. Like us, they placed no constraint on inelasticity.

Finally, we comment on the absolute magnitude of the instrumental asymmetry x_1/x_0 which mimics a polarisation asymmetry in those circumstances where it cannot be eliminated by reversing the polarisation of the incident proton. Over the period of 18 months in which we have operated the polarimeter, we have observed values of x_1/x_0 of typically ± 0.005, changing with a time constant of many hours or days. Such instrumental asymmetries can arise from the occasional dead or noise wire which has to be tolerated under practical conditions, or slow variations of chamber performance with gas composition. Since the mean analysing power, averaged over θ is typically 0.35, this instrumental asymmetry leads to an uncertainty of ± 0.015 in proton polarisation. For
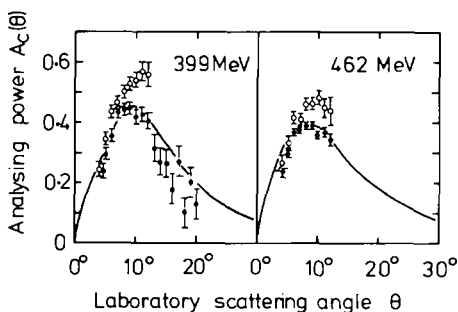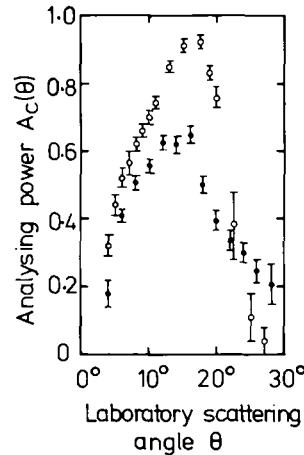

Fig. 5. Data of the Geneva group (ref. 14) compared with our empirical fit (continuous line). Energies are those of the incident protons. Solid circles refer to all events, open circles to nearly elastic events.
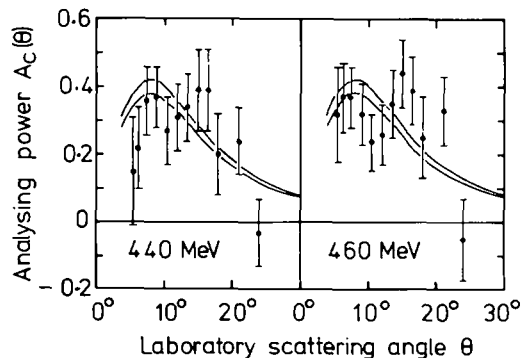

Fig. 7. Comparison of our measurements (continuous lines indicate error corridors of our empirical fit) with UCRL data (ref. 19) at the two neighbouring incident proton energies.

measurements of Wolfenstein parameters, where one is interested in changes of polarisation, this does not matter. For absolute polarisation measurements where the spin cannot be flipped, it does matter; it could presumably be greatly reduced by adding two more chambers behind the carbon, so as to increase the redundancy in the number of chambers available.

References

[1] D. Axen, L. Felawka, S. Jaccard, J. Vávra, G. A. Ludgate, N. M. Stewart, C. Amsler, R. C. Brown, D. V. Bugg, J. A. Edgington, C. J. Oram, K. Shakarchi and A. S. Clough, Lett. Nuovo Cimento 20 (1977) 151.

[2] C. Amsler, R. C. Brown, D. V. Bugg, J. A. Edgington, C. J. Oram, D. Axen, R. Dubois, L. Felawka, S. Jaccard, R. Keeler, J. Vávra, A. S. Clough, D. Gibson, G. A. Ludgate, N. M. Stewart, L. P. Robertson and J. Reginald Richardson, Nucl. Instr. and Meth. 144 (1977) 401.

[3] C. Amsler, D. Axen, J. Beveridge, D. V. Bugg, A. S. Clough, J. A. Edgington, S. Jaccard, G. A. Ludgate, C. J. Oram, J. R. Richardson. L. P. Robertson, N. M. Stewart and J. Vávra, Phys. Lett. 69B (1977) 419.

[4] C. Amsler, D. Axen, J. Beveridge, R. C. Brown, D. V. Bugg, A. S. Clough, J. A. Edgington, L. Felawka, S. Jaccard, G. A. Ludgate, C. J. Oram, J. R. Richardson, L. P. Robertson. N. M. Stewart and J. Vávra, Proc. 7th Int. Conf. High energy physics and nuclear structure, Zurich, Switzerland (1977).

[5] J. A. Edgington, Proc. 2nd Int. Conf. on Nucleon-nucleon interactions, Vancouver, Canada (1977).

[6] G. A. Ludgate, Ph. D. Thesis, University of London, England (1976) and Rutherford Laboratory Report, HEP/T/59; C. J. Oram, Ph. D. Thesis, University of London. England (1977) and Rutherford Laboratory Report, HEP/T/61.

[7] C. Amsler, D. Axen. J. Beveridge, D. V. Bugg, A. S. Clough, J. A. Edgington, D. Gibson, R. Keeler, G. A. Ludgate, C. J. Oram, J. R. Richardson, L. P. Robertson and N. M. Stewart, to be published.

[8] G. Charpak, Ann. Rev. Nucl. Sci. 20 (1970) 195; G. Charpak, R. Bouclier, T. Bressani, J. Favier and Č. Zupančič, Nucl. Instr. and Meth. 62 (1968) 262.

[9] R. Bouclier, G. Charpak, Z. Dimčovski, H. G. Fisher, F. Sauli, G. Coignet and G. Flügge, Nucl. Instr. and Meth. 88 (1970) 149.

[10] G. Charpak, H. G. Fisher, C. R. Gruhn, A. Minton, F. Sauli, G. Plch and G. Flügge, Nucl. Instr. and Meth. 99 (1972) 279.

[11] "Basque M.W.P.C. Readout System", Rutherford Laboratory Electronics Group Report, unpublished (1974).

[12] G. Gallagher-Daggit, Rutherford Laboratory Reports, RLN 74-104 (1974) and RL 75-008 (1975).

[13] T. A. Hodges, TRIUMF Report TRI-1-73-2 (1973).

[14] D. Aebischer, B. Favier. G. Greeniaus, R. Hess, A. Junod, C. Lechanoine. J. C. Niklès, D. Rapin and D. Werren, Nucl. Instr. and Meth. 124 (1975) 49.

[15] G. Coignet, CERN, Report 66-2 (1966).

[16] D. Cheng, Ph. D. Thesis, UCRL (1965).

[17] L. N. Glonti, Y. M. Kazarinov and I. K. Potashnikov, Dubna preprint P1-6362 (1972).

[18] W. G. Chesnut, Proc. 6th Ann. Rochester Conf. of High energy and nucl. phys. (Interscience Publishers Inc., New York, 1956); W. G. Chesnut, E. M. Hafner and A. Roberts. Phys. Rev. 104 (1956) 449.

[19] R. D. Eandi, R. W. Kenney and V. Z. Peterson, Nucl. Instr. and Meth. 32 (1965) 213.